

Neonatal hyperoxia induces gut dysbiosis and behavioral changes in adolescent mice

Yu-Chun Lo^a, Kai-Yun Chen^a, Hsiu-Chu Chou^b, I-Hsuan Lin^c, Chung-Ming Chen^{d,e,*}

^aThe Ph.D. Program for Neural Regenerative Medicine, College of Medical Science and Technology, Taipei Medical University, Taipei, Taiwan, ROC; ^bDepartment of Anatomy and Cell Biology, School of Medicine, College of Medicine, Taipei Medical University, Taipei, Taiwan, ROC; ^cResearch Center of Cancer Translational Medicine, Taipei Medical University, Taipei, Taiwan, ROC; ^dDepartment of Pediatrics, Taipei Medical University Hospital, Taipei, Taiwan, ROC; ^eDepartment of Pediatrics, School of Medicine, College of Medicine, Taipei Medical University, Taipei, Taiwan, ROC

Abstract

Background: Supplemental oxygen is often required to treat preterm infants with respiratory disorders. Experimental studies have demonstrated that hyperoxia results in the disruption of intestinal and neuronal plasticity and myelination of the brain. The association between the neonatal hyperoxia and changes of phenotypes in gut microbiota and in behaviors is not clear to date.

Methods: We designed an animal experiment that C57BL/6 mice pups were reared in either room air (RA) or hyperoxia (85% O₂) from postnatal days 1 to 7. From postnatal days 8 to 42, the mice were reared in RA. Intestinal microbiota was sampled from the lower gastrointestinal tract on postnatal days 7 and 42, and behavioral tests were performed and brain tissues were collected on postnatal day 42.

Results: Neonatal hyperoxia decreased intestinal tight junction protein expression and altered intestinal bacterial composition and diversity on postnatal day 7. Among the concrete discriminative features, *Proteobacteria* and *Epsilonbacteraeota* were significantly elevated in hyperoxia-reared mice on postnatal days 7 and 42, respectively. Hyperoxia-reared mice exhibited significantly reduced sociability and interest in social novelty and impaired motor coordination compared with RA-reared mice on postnatal day 42. Hyperoxia-reared mice also exhibited significantly reduced myelination and a significantly higher number of apoptotic cells in the brain compared with RA-reared mice on postnatal day 42.

Conclusion: Neonatal hyperoxia during the first week of life altered gut microbiota and reduced brain myelination that might associate with the deficits of social interaction and motor coordination in adolescent mice.

Keywords: Gut microbiota; Motor coordination; Neonatal hyperoxia; Sociability

1. INTRODUCTION

Premature birth is the leading cause of death for children under 5 years, and the estimated global prevalence ranges from 5% to 18%.¹ Improvements in neonatal respiratory care have increased the survival rate of infants with very low birth weight.² Supplemental oxygen is often required to treat newborns with respiratory disorders. However, the oxygen therapy provided to infants has beneficial and adverse effects. Supraphysiologic oxygen concentrations have harmful effects on the developing brain and lead to neuronal cell death and contribute to brain injury in preterm infants.³ Despite major advances in neonatal

intensive care, preterm infants who survive frequently have neurodevelopmental impairments in later life. Clinical studies have demonstrated that hyperoxia increases the risk of delayed neurobehavioral and cognitive effects and the development of cerebral palsy in preterm infants.^{4,5}

Preterm neonates are often vulnerable to injury caused by reactive oxygen species owing to the immaturity of their endogenous radical scavenging systems.⁶ Experimental studies have revealed that hyperoxia alters developmental processes and results in the disruption of neural plasticity and myelination during the critical phase of brain maturation.^{7,8} A substantial proportion of premature infants still have neurologic deficits, which affect motor and cognitive function in childhood.^{9–11} Even in the absence of apparent intracranial pathology, such as intraventricular hemorrhage or periventricular leukomalacia, preterm infants have a high risk of neurodevelopmental impairment.

Microbiota of the intestinal tract has been implicated in regulation of inflammatory, infectious and metabolic diseases and plays a critical role in maintaining human health.¹² Recently, the interaction between brain and gut microbiota has been investigated in different populations, including neurodevelopment disorders,¹³ neurodegenerative disorders,¹⁴ and metabolism syndromes.¹⁵ The neural signaling via the autonomic nervous system to the gut might cause the change of microbiota distribution and activity.¹⁶ On the other hand, metabolic production of microbiota was carried and absorbed by the blood system then

*Address correspondence. Dr. Chung-Ming Chen, Department of Pediatrics, School of Medicine, College of Medicine, Taipei Medical University, 250, Wu-Hsing Street, Taipei 110, Taiwan, ROC. E-mail address: cmchen@tmu.edu.tw (C.-M. Chen).

Author Contributions: Dr. Yu-Chun Lo and Dr. Kai-Yun Chen contributed equally to this work.

Conflicts of interest: The authors declare that they have no conflicts of interest related to the subject matter or materials discussed in this article.

Journal of Chinese Medical Association. (2021) 84: 290-298.

Received September 10, 2020; accepted December 10, 2020.

doi: 10.1097/JCMA.0000000000000488.

Copyright © 2021, the Chinese Medical Association. This is an open access article under the CC BY-NC-ND license (<http://creativecommons.org/licenses/by-nc-nd/4.0/>)

Table 1
Body weight on postnatal days 7 and 42 in the room air- or hyperoxia-reared mice

Treatment	n	Body weight on postnatal day 7 (g)	n	Body weight on postnatal day 42 (g)
Room air	11	3.28 ± 0.56	14	18.03 ± 2.03
Hyperoxia	7	2.64 ± 0.41 ^a	7	15.65 ± 2.31 ^a

Values are presented as mean ± SD.
^a*p* < 0.05, compared with the room air group.

effect brain regulation.¹⁷ Evidence suggests that the influence of host-microbe interactions may extend beyond the local environment and influence peripheral tissues.¹⁸ Previous study has identified hyperoxia-increased epithelial permeability and translocation of bacteria from the gastrointestinal tract to the internal organs.¹⁹ However, the association between changes of gut microbiome and the pathogenesis of brain diseases in newborns and adolescents after neonatal hyperoxia exposure is not clear

to date. This study investigated the association between neonatal hyperoxia and the alterations of intestinal microbiota as well as the brain development in newborn and adolescent mice.

2. METHODS

2.1. Experimental groups

We conducted the experiments in accordance with approved guidelines and regulations of the Institutional Animal Care and Use Committee of Taipei Medical University (LAC-2019-0290). Time-dated pregnant C57BL/6N mice were purchased from Bio-LASCO Taiwan Co., Ltd., Nangang Dist., Taipei and they were housed in individual cages with free access to laboratory food and water. Within 12 hours of birth, the litters were pooled and randomly redistributed among the newly delivered mothers based on the body weight stratification, and the pups were then randomly assigned to be reared in room air (RA) at 21% O₂ or O₂-enriched air (85%). The pups in the hyperoxia group were reared in an atmosphere containing 85% O₂ for postnatal days 1 to 7, which represents the sacular stage in mice and mimic the supplemental oxygen exposure used for human neonates.²⁰

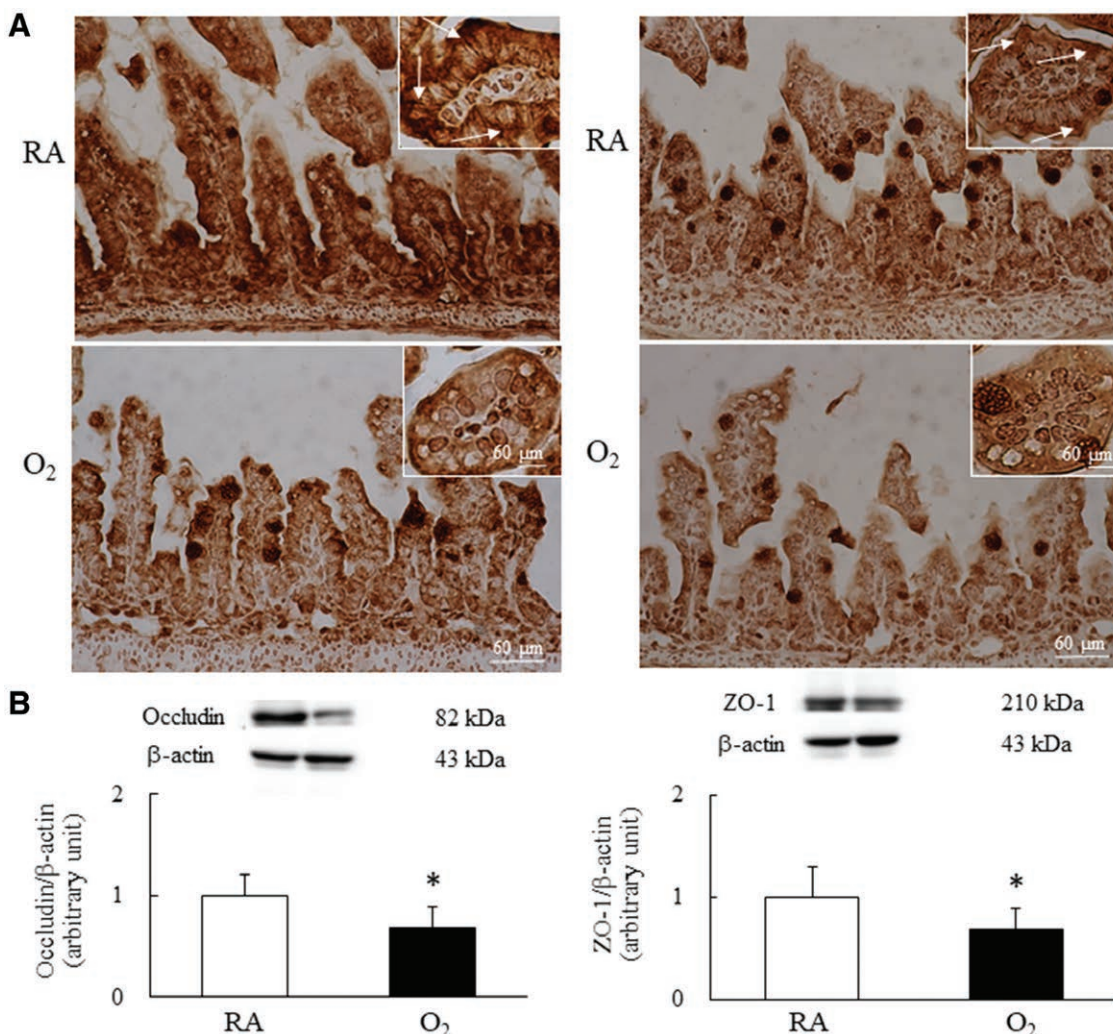


Fig. 1 A, Representative immunohistochemistry and (B) Western blotting of tight junction proteins in the ileum of RA- and hyperoxia-reared mice on postnatal day 7. Occludin and ZO-1 were observed on the side adjacent to the cell membranes of the enterocytes. The RA-reared mice exhibited intact construct of occludin and ZO-1 staining. The hyperoxia-reared mice exhibited disrupted occludin and ZO-1 immunohistochemistry. The hyperoxia-reared mice exhibited significantly lower occludin and ZO-1 protein levels than RA-reared mice did. n = 7–11 mice per group. **p* < 0.05 vs RA group. RA = room air.

To avoid O₂ toxicity in the nursing mothers, they were rotated between the O₂ treatment and RA control litters every 24 hours.

On postnatal day 7, 11 and seven mice were allocated haphazardly from four RA cages and four hyperoxia cages respectively for collecting tissues and intestinal microbiota samples. Rest of the mice were reared in RA from postnatal days 8 to 42. On postnatal day 21, 14 mice (eight males and six females in the RA cages) and seven mice (four males and three females in the hyperoxia cages) were haphazardly allocated to eight cages. We evaluated sociability in adolescent mice as mice progress through a period of adolescence characterized by behaviors such as increased risk-taking and social play²¹ on postnatal day 42. Then mice were sacrificed after being anesthetized to unconscious with 2.5% isoflurane in an anesthesia chamber according to the guidelines for euthanasia and their tissues and samples of intestinal microbiota were harvested.

2.2. Behavioral tests

The three-chamber social test involving an unfamiliar mouse with the experimental mouse was performed on both groups according to the Crawley study.²² The social interaction test was conducted during the light cycle in a 60 × 30 × 30 cm³ behavioral box, which included three chambers, namely empty, central, and social chambers. Each experimental mouse was first placed in the central chamber for 10 minutes to acquire its tropism and

then was moved out from the behavioral box. Then, a stranger mouse with matched sex and age to the experimental mouse was randomly selected and placed inside a small cage in the social chamber, which prevented its direct contact with the experimental mouse. Next, the experimental mouse was placed into the behavioral box again for 10 minutes. The time spent in each chamber was recorded from a camera mounted overhead, analyzed by an automated tracking program, and calculated using the following equation: Chamber duration rate (%) = stay time/total time × 100%.

In the beam-walking test, mice were placed on a Plexiglas beam (7 mm wide, 110 cm length) elevated 30 cm above the bench by metal supports to a goal box.²³ Two permanent markers marked the start line and finish line, with a distance between them of 80 cm. Recording commenced when the mouse's forelimbs reached the start line and stopped when the mouse reached the finish line. Mice that fell were returned to the position they fell from, with a maximum time of 60 seconds allowed on the beam. The beam-walking test was conducted with experimental mice for 5 days (eight trials each day), and the result on the fifth day was considered the baseline in this study.

2.3. Brain tissue collection

On postnatal day 42, mice were deeply anesthetized through an overdose of isoflurane and were transcardially perfused with

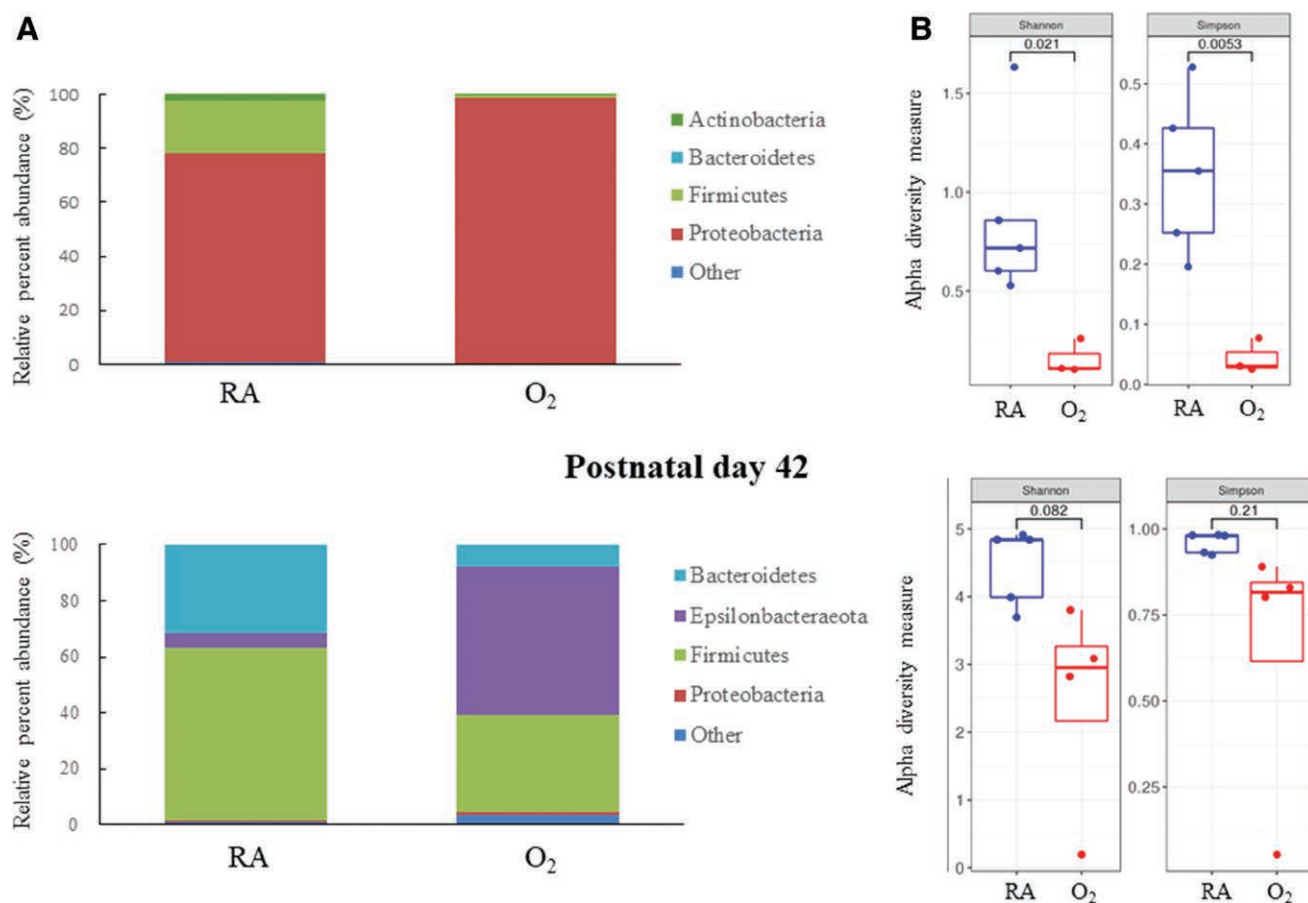


Fig. 2 A, Relative phylum-level abundance of bacteria and (B) diversity in the intestine on postnatal days 7 and 42. Each bar represents the community of one group and the different taxa are represented by different colors. On postnatal day 7, most samples were dominated by *Proteobacteria* (98.7%) in the intestine of hyperoxia-exposed mice and *Firmicutes* (19.6%) in the intestine of RA-exposed mice. On postnatal day 42, the majority of samples were dominated by *Epsilonbacteraeota* (53.1%) in the intestine of hyperoxia-exposed mice and *Firmicutes* (61.8%) in the intestine of RA-exposed mice. Hyperoxia-reared mice exhibited significantly decreased alpha diversity compared with RA-reared mice on postnatal day 7, whereas diversity was not significantly different between the RA and hyperoxia groups on postnatal day 42. n = 4–6 mice per group. RA = room air.

8 mL of ice-cold phosphate-buffered saline followed by 4% paraformaldehyde. Brains were removed and postfixed in 4% paraformaldehyde overnight at 4°C and then embedded in paraffin. Five-micrometer coronal sections of brain corresponding to 2.12–2.3 mm from the bregma were cut.

2.4. In situ apoptosis analysis

A commercial in situ apoptosis detection kit (ab206386; Abcam, Cambridge, MA) was used to detect apoptosis in the sections. Apoptotic cells were labeled with terminal deoxynucleotidyl transferase, which catalyzes the addition of biotin-labeled deoxynucleotides. Positive signals were detected using 3,3'-diaminobenzidine substrate and visualized according to brown labels. The slides were then counterstained with methyl green.²⁴ The degenerated oligodendrocytes and neurons were quantified by counting the positive brown labeled cells in five randomly selected fields of

each section of cerebrum at 400× magnification using an Olympus BX43 microscope (Olympus Corporation, Tokyo, Japan).

2.5. Immunohistochemistry

The sections were incubated with rabbit polyclonal antimyelin basic protein (MBP) and antizonula occludens (ZO)-1 antibodies (MBP 1:100; Abcam, ZO-1 1:50; Santa Cruz Biotechnology, Inc., Dallas, TX) and mouse monoclonal anti-occludin (1:50 dilution; Santa Cruz Biotechnology, Inc.) as primary antibodies. The sections were treated with biotinylated goat anti-rabbit IgG (1:200; Jackson ImmunoResearch Laboratories Inc., PA, USA) for the MBP and ZO-1 antibodies and with biotinylated rabbit antimouse IgG for the occludin antibody (1:200; Jackson ImmunoResearch Laboratories Inc.), followed by a reaction with reagents from an avidin–biotin complex kit (Vector Laboratories Inc., Burlingame, CA). The mean optical density values of the MBP, ZO-1, and occludin-positive staining in the

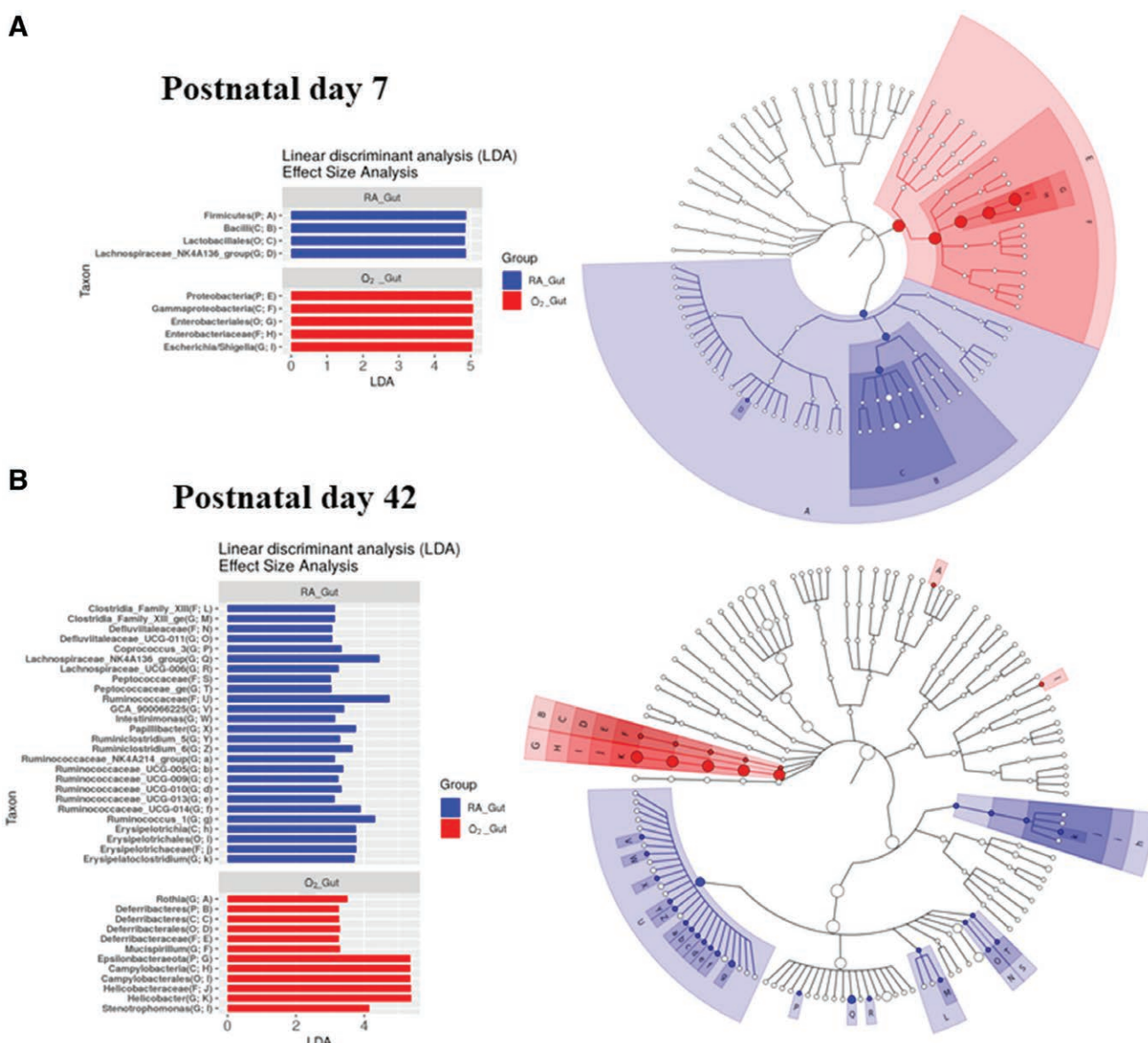


Fig. 3 Histogram of the LDA scores and the cladogram in the intestine on postnatal days 7 and 42 revealed the most differentially abundant taxa in the two groups. The microbiome distribution was compared between RA and O₂ groups by using linear discriminant analysis effect size. The cladogram illustrates the significantly overrepresented bacterial taxa in the RA group (blue area) and O₂ group (red area). n = 7–11 mice per group. LDA = linear discriminant analysis; RA = room air.

cerebrum and thalamus of each section at 400× magnification was recorded using the Image-Pro Plus software package (Media Cybernetics, Silver Spring, MD).

2.6. Western blot analysis of intestinal occludin and ZO-1

Intestine tissues were homogenized and the membranes were incubated with anti-occludin (Santa Cruz Biotechnology, Inc., CA), anti-ZO-1 (750; Santa Cruz Biotechnologies, Inc.), or anti- β -actin (1:1000; Santa Cruz Biotechnologies, Inc.) Protein bands were detected using BioSpectrum AC System (UVP, Upland, CA).

2.7. Intestinal bacteria DNA collection and extraction

After the mice were sacrificed, 2 cm of the lower gastrointestinal tract from the anus to the colon of the mice at the age of 1- and 6-week was dissected to extract DNA for bacterial analysis. After dissection, the tissue including the intestinal wall and the intestinal content was immediately used to perform intestinal bacteria DNA extraction using QIAamp PowerFecal DNA commercial kits (QIAGEN, Hilden, German) following the manufacturer's instructions.

2.8. 16S rRNA gene sequence analysis

After sequencing, universal primer sequences and low-quality reads were trimmed using cutadapt (v1.15),²⁵ and processed and analyzed with the DADA2/phyloseq workflow in the R environment. Briefly, filtering, trimming, dereplication, and denoising of the forward and reversed reads were performed using the DADA2 package (v1.6).²⁶ Processed overlapping paired-end reads were merged and chimeras were subsequently removed from the cleaned full-length amplicons. Taxonomy assignment of the inferred amplicon sequence variants (ASVs) was performed using the SILVA reference database (v132)²⁷ with a minimum bootstrap confidence of 80. Multiple sequence alignment of the ASVs was performed with DECIPHER package (v2.6.0)²⁸ and

the phylogenetic tree was constructed using RAxML (v8.2.11).²⁹ The frequency table, taxonomy, and phylogenetic tree information were used to create a phyloseq object for downstream bacterial community analyses using the phyloseq package (v1.22.3).³⁰

2.9. Statistical analysis

Data were expressed as mean \pm SD. Between group comparisons of each age group were conducted using Student's *t*-test. Differences were considered significant at $p < 0.05$. For the social interaction comparison and the beam-walking test, a Wilcoxon two-sample *t*-test was performed to compare the differences between the RA and hyperoxia groups, and the significance level was set at $p < 0.05$. Bacterial compositions among samples were visualized using bar plots. Alpha diversity indices were calculated using the estimate richness function from the phyloseq package, and a two-tailed Student's *t*-test was performed to compare the alpha diversity indices between groups. Microbiota enrichment analysis between groups was conducted using the linear discriminant analysis (LDA) effect size method, with alpha set at 0.05 (Kruskal-Wallis and Wilcoxon tests) and a logarithmic LDA score of 3 or more;³¹ the analysis was visualized as a cladogram by using GraPhlAn.³²

3. RESULTS

Mice reared in a hyperoxic environment from postnatal days 1 to 7 exhibited considerably lower body weights when compared, on postnatal days 7 and 42, with mice reared in RA (Table).

Immunohistochemistry and Western blotting for occludin and ZO-1 are presented in Fig. 1. Both occludin and ZO-1 were observed on the side adjacent to the cell membranes of the enterocytes. We observed a continuous and intact construct of occludin and ZO-1 staining in the RA-reared mice (Fig. 1A). The hyperoxia-reared mice exhibited disrupted occludin and

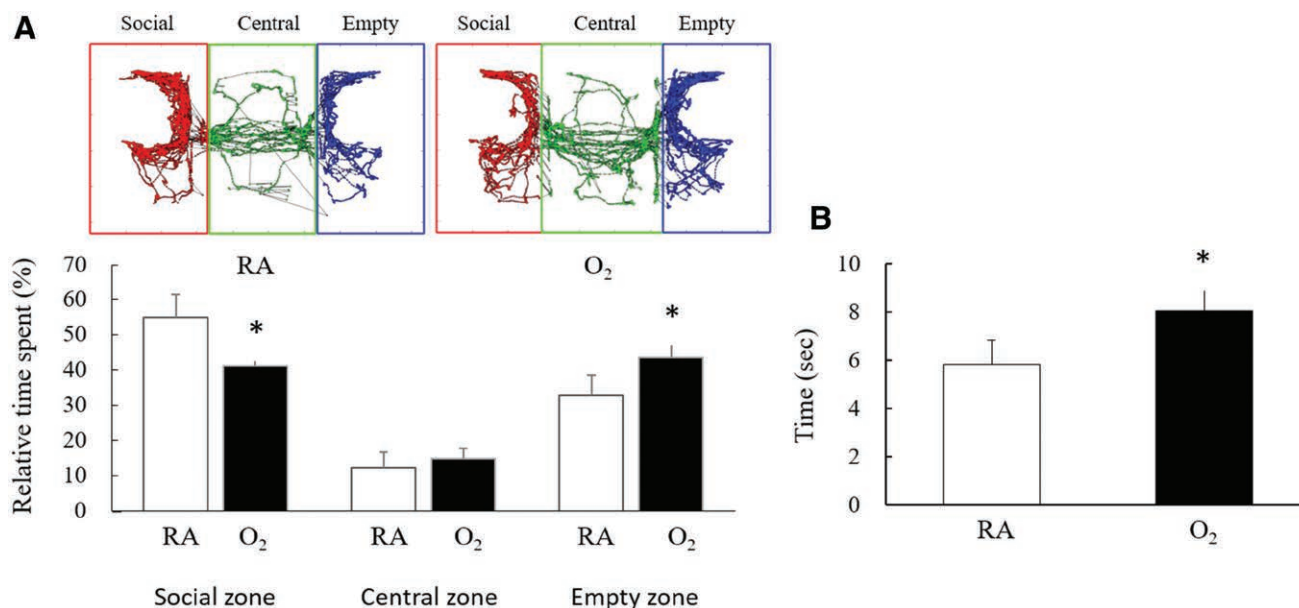


Fig. 4 A, Sociability assessed by the three-chamber test and (B) motor coordination and balance analyzed by the beam-walking test on postnatal day 42. The time spent in each chamber was recorded from a camera mounted overhead, analyzed by an automated tracking program, and calculated using the following equation: chamber duration rate (%) = stay time/total time \times 100%. The first, the second, and the third sets of bars in (A) represented the chamber duration rate in the social zone, central zone, and empty zone, respectively. Mice reared in a hyperoxic environment for the first week of life spent more time in the empty chamber when compared with the mice reared in a RA environment. Mice reared in RA spent more time to investigate the activities of the novel stranger mouse, whereas mice reared in hyperoxia spent more time to investigate the empty zone. Hyperoxia-reared mice required significantly more time to transverse the beam compared with RA-reared mice. $n = 4-6$ mice per group. * $p < 0.05$ vs RA group. RA = room air.

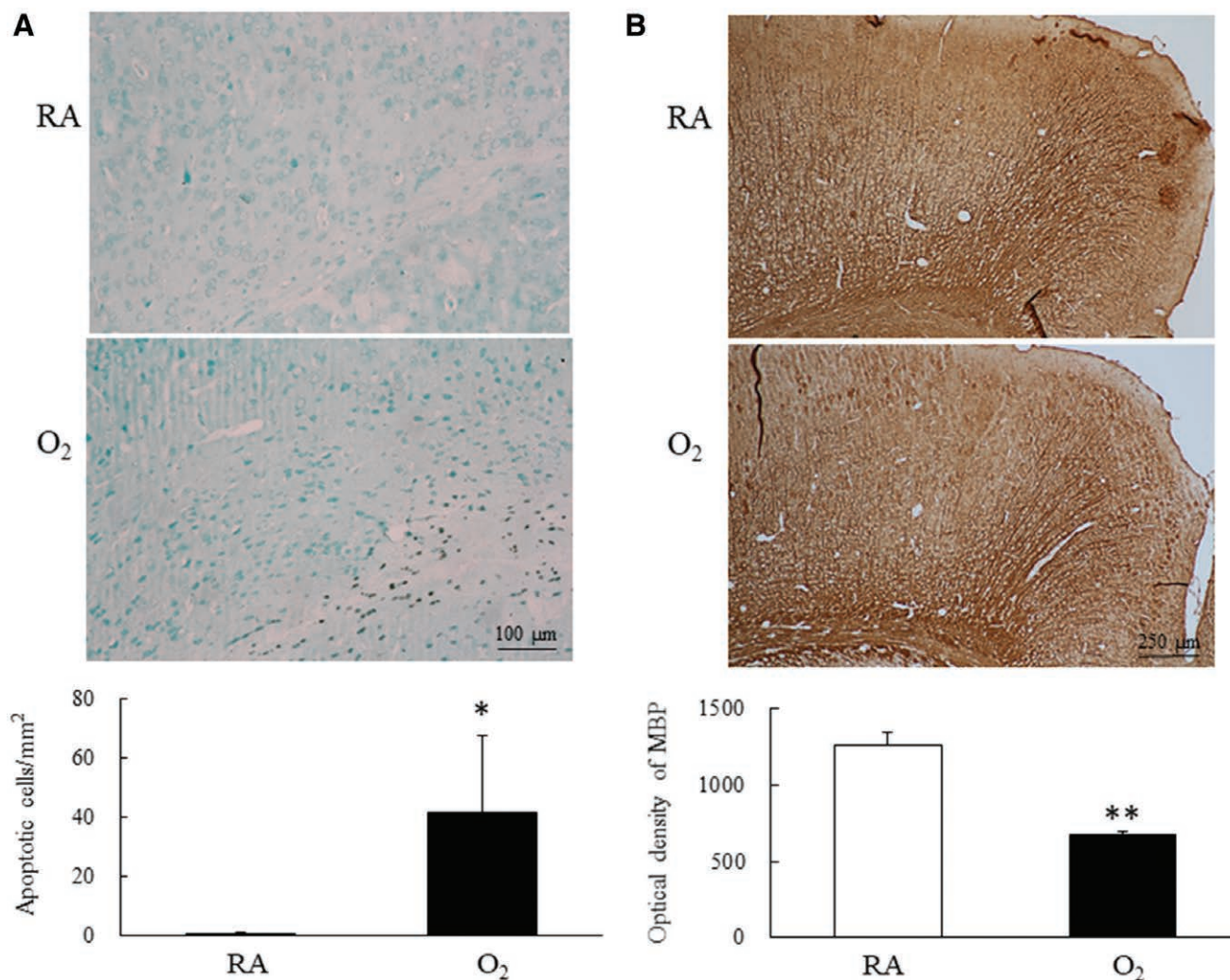


Fig. 5 A, Representative apoptotic staining and (B) immunohistochemistry of MBP in brain sections and semiquantitative measurement of apoptotic cells and MBP immunoreactivity on postnatal day 42. Positive staining was observed in the cell nuclei and shown in brown (arrows). The hyperoxia-reared mice exhibited a significantly higher number of apoptotic cells than that observed in the RA-reared mice. MBP expression was mainly localized in the processes (nerve fibers) and soma of neurons (arrows). The hyperoxia-reared mice exhibited more intense MBP immunoreactivity than that observed in the RA-reared mice. The semiquantitative analysis revealed that neonatal hyperoxia significantly increased MBP immunoreactivity compared with RA rearing in mice on postnatal day 42. $n = 5$ mice per group. * $p < 0.05$, ** $p < 0.01$ vs RA group. MBP = myelin basic protein; RA = room air.

ZO-1 immunohistochemistry between adjacent enterocytes and considerably lower occludin and ZO-1 protein levels than those of the RA-reared mice (Fig. 1B).

We analyzed the taxonomical community structure of the gut microbiome of mice to determine the response to hyperoxia on postnatal day 7 (Fig. 2A). At the phylum level, all samples from the RA and hyperoxia groups contained *Actinobacteria*, *Bacteroidetes*, *Firmicutes*, and *Proteobacteria*. Relative abundances of *Firmicutes* and *Proteobacteria* significantly differed between the RA and hyperoxia groups (Fig. 2A). On postnatal day 42, all samples from the RA and hyperoxia groups contained *Bacteroidetes*, *Epsilonbacteraeota*, *Firmicutes*, and *Proteobacteria* at the phylum level. The relative abundance of *Epsilonbacteraeota* significantly differed between two groups. Moreover, the alpha diversity was analyzed to compare the microbiome richness between two groups, and the Shannon and Simpson indices were calculated on postnatal days 7 and 42, respectively. Hyperoxia-reared mice exhibited significantly decreased alpha diversity compared with RA-reared mice on postnatal day 7, whereas diversity was not significantly

different between the RA and hyperoxia groups on postnatal day 42 (Fig. 2B).

Furthermore, on postnatal day 7, a total of nine taxa had significantly different abundances between the groups (LDA score >3.0). Four microbial taxa were enriched in the RA group compared with the hyperoxia group. The hyperoxia group was characterized by a higher abundance of five other discriminatory taxa (Fig. 3A). On postnatal day 42, 38 taxa manifested significant differences in their abundance between the groups (LDA score >3.0). Twenty-six microbial taxa had higher enrichment in the RA group than in the hyperoxia group. The hyperoxia group was characterized by a higher abundance of 12 other discriminatory taxa (Fig. 3B).

We performed the three-chamber test to examine the sociability of the mice on postnatal day 42 (Fig. 4A). The hyperoxia-reared mice exhibited a significantly shorter ratio of social chamber duration time ($41.3\% \pm 4.1\%$) than did the RA-reared mice ($54.9\% \pm 6.7\%$, $p < 0.05$). The ratio of chamber duration time in the empty chamber was $32.9\% \pm 5.7\%$ and $43.7\% \pm 6.7\%$ in the RA and hyperoxia groups, respectively. Mice

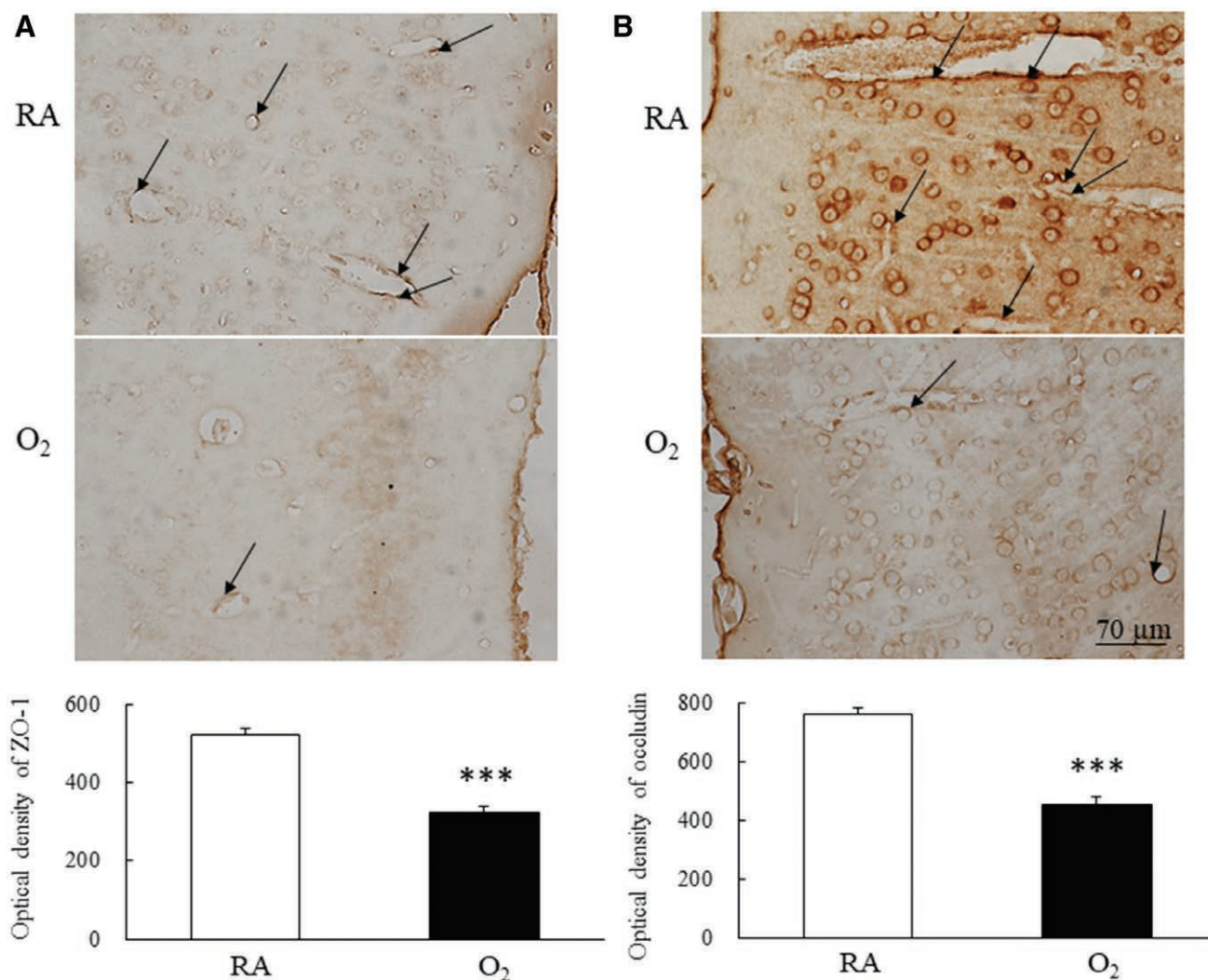


Fig. 6 Representative immunohistochemistry of (A) ZO-1 and (B) occludin in brain sections and semiquantitative measurement of ZO-1 and occludin immunoreactivity on postnatal day 42. The hyperoxia-reared mice exhibited more ZO-1 (black arrow) and occludin (black arrow) immunoreactivity than that observed in the RA-reared mice. The semiquantitative analysis revealed that neonatal hyperoxia significantly decreased ZO-1 and occludin immunoreactivity compared with RA rearing mice on postnatal day 42. $n = 5$ mice per group. *** $p < 0.001$ vs RA group. RA = room air.

reared in RA spent more time investigating the activities of the novel stranger mouse, whereas mice reared in hyperoxia tended to avoid the social interaction with the novel stranger mouse. Moreover, hyperoxia-reared mice required significantly more time to transverse the beam compared with RA-reared mice (Fig. 4B, $p < 0.05$).

In RA-reared mice, we observed almost no staining in the brain sections. The apoptotic cells were stained brown in the cell nuclei (Fig. 5A). The hyperoxia-reared mice exhibited a significantly higher number of apoptotic cells in the cerebrum and thalamus than did the RA-reared mice ($p < 0.05$). Immunohistochemistry staining of MBP was performed on the mouse brains to investigate myelination. MBP expression was mainly localized in the processes (nerve fibers) and soma of neurons (Fig. 5B), and the fine MBP-positive fibers were scattered throughout the adjacent cortex. The hyperoxia-reared mice exhibited more intense MBP immunoreactivity than did the RA-reared mice ($p < 0.01$).

The hyperoxia-reared mice exhibited more ZO-1 and occludin immunoreactivity than that observed in the RA-reared mice (Fig. 6). The semiquantitative analysis revealed that neonatal hyperoxia significantly decreased ZO-1 and occludin

immunoreactivity compared with RA rearing mice on postnatal day 42.

4. DISCUSSION

Our *in vivo* model revealed that exposure of neonatal mice to hyperoxia is related to the change of gut bacterial composition in newborn and adolescent mice. Hyperoxia might alter phenotypes of brain myelination, sociability, and motor coordination in adolescent mice. The development of neonatal hyperoxia-induced gut dysbiosis was associated with reduced social interaction and impaired motor coordination and that gut dysbiosis precedes behavioral changes. The gut microbiota has been reported to influence blood-brain barrier permeability and brain and social development in mice.^{33–36} These results suggest that the gut microbiota might be related to the pathogenesis of hyperoxia-induced brain damage and behavioral changes.

The brain of a rodent pup is similar structurally to the brain of a human preterm infant born at 24–28 weeks of gestation and is used to study the mechanisms of perinatal brain damage.³⁷ In rodents with short gestation periods such as rats and

the intestine is relatively immature at birth and for the first 2 postnatal weeks.³⁸ Therefore, newborn mice are useful models for studies of brain and intestine injury. During the first week period of hyperoxia, the body weight of hyperoxia-reared mice was reduced to 80% of that of the RA-reared controls. The body weight reduction effect of neonatal hyperoxia extended to postnatal day 42 after mice returned to a RA atmosphere from postnatal day 8. These results suggest that neonatal hyperoxia has persistent and delayed effects on growth.

A microbiota is an ecologic community of commensal, symbiotic, and pathogenic microorganisms found in and on all multicellular organisms from plants to animals.¹⁸ A healthy gut microbiota is essential for human health.³⁹ We revealed that newborn mice exposed to hyperoxia exhibited decreased bacterial diversity on postnatal day 7 and different gut microbiota compositions on postnatal days 7 and 42. Hyperoxia-reared mice had significantly decreased intestinal tight junction and displayed significantly higher *Proteobacteria* abundance compared with RA-reared mice on postnatal day 7. These results were consistent with the finding that a higher relative abundance of *Proteobacteria* increases intestinal permeability in mice.⁴⁰ Our findings implied that the gut dysbiosis preceded the development of reduced social interaction and impaired motor coordination.

Adolescent and young adult mice exposed to hyperoxia as newborn mice exhibited hyperactivity and motor coordination deficits and abnormal neurobehavior deficits in spatial navigation, recognition, and memory.^{41–43} We demonstrated that after neonatal hyperoxia, adolescent mice had lower levels of sociability and diminished preference for social novelty compared with adolescent mice reared in neonatal RA. We also employed the beam-walking pattern to detect fine motor coordination through a spontaneous motor task.⁴⁴ Motor impairment related to ataxic and dystonic characteristics can be assessed based on the animal's difficulty in crossing beams and cross-sectional areas.⁴⁵ We found that neonatal hyperoxia resulted in adolescent mice having poor behavioral performance which indicate that neonatal hyperoxia may induce ataxia and dystonia in mice during adolescence.

Preclinical studies have demonstrated that exposure to hyperoxia disrupts myelin formation and induces apoptosis in the brains of newborn animals.³ The effects of neonatal hyperoxia on myelination in adolescents was unknown. We found decreased MBP expression in murine brains on postnatal day 42. Our findings were compatible with those of Serdar et al²⁴ who observed several myelin abnormalities, including increased nonmyelinated axons and adaxonal space in 6-week-old mice following neonatal hyperoxia on postnatal day 6. Myelination is active in preterm infants and during the early postnatal period in rodents.⁴⁶ These results suggest that neonatal hyperoxia may lead to impaired memory function in adolescents and adults.

The exposure of neonatal mice to hyperoxia for the first week of life altered the gut microbial composition which continuing to the adolescent periods and reduced brain myelination that might associate with the deficits of social interaction and motor coordination in adolescent mice. Further investigation of the role of the gut–brain axis may offer new treatment strategies for hyperoxia-induced brain injury.

ACKNOWLEDGMENTS

This work was supported by a grant from the Ministry of Science and Technology of Taiwan (MOST-109-2314-B-078-073).

We would like to acknowledge the technologic and analysis support provided by TMU Core Laboratory of Human Microbiome.

REFERENCES

1. Chawanpaiboon S, Vogel JP, Moller AB, Lumbiganon P, Petzold M, Hogan D, et al. Global, regional, and national estimates of levels of preterm birth in 2014: a systematic review and modelling analysis. *Lancet Glob Health* 2019;7:e37–46.
2. Su YY, Wang SH, Chou HC, Chen CY, Hsieh WS, Tsao PN, et al; Taiwan Premature Infant Follow-up Network. Morbidity and mortality of very low birth weight infants in Taiwan—Changes in 15 years: a population based study. *J Formos Med Assoc* 2016;115:1039–45.
3. Reich B, Hoerber D, Bendix I, Felderhoff-Mueser U. Hyperoxia and the Immature Brain. *Dev Neurosci* 2016;38:311–30.
4. Collins MP, Lorenz JM, Jetton JR, Paneth N. Hypocapnia and other ventilation-related risk factors for cerebral palsy in low birth weight infants. *Pediatr Res* 2001;50:712–9.
5. Deulofeut R, Dudell G, Sola A. Treatment-by-gender effect when aiming to avoid hyperoxia in preterm infants in the NICU. *Acta Paediatr* 2007;96:990–4.
6. Perrone S, Tataranno LM, Stazzoni G, Ramenghi L, Buonocore G. Brain susceptibility to oxidative stress in the perinatal period. *J Matern Fetal Neonatal Med* 2015;28(Suppl 1):2291–5.
7. Du M, Tan Y, Liu G, Liu L, Cao F, Liu J, et al. Effects of the Notch signaling pathway on hyperoxia-induced immature brain damage in newborn mice. *Neurosci Lett* 2017;653:220–7.
8. Endesfelder S, Makki H, von Haefen C, Spies CD, Bühner C, Sifringer M. Neuroprotective effects of dexmedetomidine against hyperoxia-induced injury in the developing rat brain. *PLoS One* 2017;12:e0171498.
9. Marlow N, Wolke D, Bracewell MA, Samara M; EPICure Study Group. Neurologic and developmental disability at six years of age after extremely preterm birth. *N Engl J Med* 2005;352:9–19.
10. Oskoui M, Coutinho F, Dykeman J, Jetté N, Pringsheim T. An update on the prevalence of cerebral palsy: a systematic review and meta-analysis. *Dev Med Child Neurol* 2013;55:509–19.
11. Wood NS, Costeloe K, Gibson AT, Hennessy EM, Marlow N, Wilkinson AR; EPICure Study Group. The EPICure study: associations and antecedents of neurological and developmental disability at 30 months of age following extremely preterm birth. *Arch Dis Child Fetal Neonatal Ed* 2005;90:F134–40.
12. Tamburini S, Shen N, Wu HC, Clemente JC. The microbiome in early life: implications for health outcomes. *Nat Med* 2016;22:713–22.
13. Sharon G, Cruz NJ, Kang DW, Gandal MJ, Wang B, Kim YM, et al. Human Gut microbiota from autism spectrum disorder promote behavioral symptoms in mice. *Cell* 2019;177:1600–18.e17.
14. Xu R, Wang Q. Towards understanding brain-gut-microbiome connections in Alzheimer's disease. *BMC Syst Biol* 2016;10(Suppl 3):63.
15. Soto M, Herzog C, Pacheco JA, Fujisaka S, Bullock K, Clish CB, et al. Gut microbiota modulate neurobehavior through changes in brain insulin sensitivity and metabolism. *Mol Psychiatry* 2018;23:2287–301.
16. Tsurugizawa T, Uematsu A, Nakamura E, Hasumura M, Hirota M, Kondoh T, et al. Mechanisms of neural response to gastrointestinal nutritive stimuli: the gut-brain axis. *Gastroenterology* 2009;137:262–73.
17. Valles-Colomer M, Falony G, Darzi Y, Tigchelaar EF, Wang J, Tito RY, et al. The neuroactive potential of the human gut microbiota in quality of life and depression. *Nat Microbiol* 2019;4:623–32.
18. Amon P, Sanderson I. What is the microbiome? *Arch Dis Child Educ Pract Ed* 2017;102:257–60.
19. Chou HC, Chen CM. Neonatal hyperoxia disrupts the intestinal barrier and impairs intestinal function in rats. *Exp Mol Pathol* 2017;102:415–21.
20. Berger J, Bhandari V. Animal models of bronchopulmonary dysplasia. The term mouse models. *Am J Physiol Lung Cell Mol Physiol* 2014;307:L936–47.
21. Laviola G, Macrì S, Morley-Fletcher S, Adriani W. Risk-taking behavior in adolescent mice: psychobiological determinants and early epigenetic influence. *Neurosci Biobehav Rev* 2003;27:19–31.
22. Crawley JN. Designing mouse behavioral tasks relevant to autistic-like behaviors. *Ment Retard Dev Disabil Res Rev* 2004;10:248–58.
23. Stanley JL, Lincoln RJ, Brown TA, McDonald LM, Dawson GR, Reynolds DS. The mouse beam walking assay offers improved sensitivity over the mouse rotarod in determining motor coordination deficits induced by benzodiazepines. *J Psychopharmacol* 2005;19:221–7.
24. Serdar M, Herz J, Kempe K, Winterhager E, Jastrow H, Heumann R, et al. Protection of oligodendrocytes through neuronal overexpression of the small GTPase ras in hyperoxia-induced neonatal brain injury. *Front Neurol* 2018;9:175.

25. Martin M. Cutadapt removes adapter sequences from high-throughput sequencing reads. *EMBnet J* 2011;17:10–2.
26. Callahan BJ, McMurdie PJ, Rosen MJ, Han AW, Johnson AJ, Holmes SP. DADA2: high-resolution sample inference from Illumina amplicon data. *Nat Methods* 2016;13:581–3.
27. Quast C, Pruesse E, Yilmaz P, Gerken J, Schweer T, Yarza P, et al. The SILVA ribosomal RNA gene database project: improved data processing and web-based tools. *Nucleic Acids Res* 2013;41(Database issue):D590–6.
28. Wright ES. DECIPHER: harnessing local sequence context to improve protein multiple sequence alignment. *BMC Bioinformatics* 2015;16:322.
29. Stamatakis A. RAxML version 8: a tool for phylogenetic analysis and post-analysis of large phylogenies. *Bioinformatics* 2014;30:1312–3.
30. McMurdie PJ, Holmes S. phyloseq: an R package for reproducible interactive analysis and graphics of microbiome census data. *PLoS One* 2013;8:e61217.
31. Segata N, Izard J, Waldron L, Gevers D, Miropolsky L, Garrett WS, et al. Metagenomic biomarker discovery and explanation. *Genome Biol* 2011;12:R60.
32. Asnicar F, Weingart G, Tickle TL, Huttenhower C, Segata N. Compact graphical representation of phylogenetic data and metadata with GraPhlAn. *PeerJ* 2015;3:e1029.
33. Braniste V, Al-Asmakh M, Kowal C, Anuar F, Abbaspour A, Tóth M, et al. The gut microbiota influences blood-brain barrier permeability in mice. *Sci Transl Med* 2014;6:263ra158.
34. Desbonnet L, Clarke G, Shanahan F, Dinan TG, Cryan JF. Microbiota is essential for social development in the mouse. *Mol Psychiatry* 2014;19:146–8.
35. Lu J, Synowiec S, Lu L, Yu Y, Bretherick T, Takada S, et al. Microbiota influence the development of the brain and behaviors in C57BL/6J mice. *PLoS One* 2018;13:e0201829.
36. Warner BB. The contribution of the gut microbiome to neurodevelopment and neuropsychiatric disorders. *Pediatr Res* 2019;85:216–24.
37. Semple BD, Blomgren K, Gimlin K, Ferriero DM, Noble-Haeusslein LJ. Brain development in rodents and humans: identifying benchmarks of maturation and vulnerability to injury across species. *Prog Neurobiol* 2013;106-107:1–16.
38. Henning SJ. Postnatal development: coordination of feeding, digestion, and metabolism. *Am J Physiol* 1981;241:G199–214.
39. Cryan JF, Dinan TG. Gut microbiota: microbiota and neuroimmune signalling-Metchnikoff to microglia. *Nat Rev Gastroenterol Hepatol* 2015;12:494–6.
40. Jakobsson HE, Rodríguez-Piñero AM, Schütte A, Ermund A, Boysen P, Bemark M, et al. The composition of the gut microbiota shapes the colon mucus barrier. *EMBO Rep* 2015;16:164–77.
41. Ramani M, van Groen T, Kadish I, Ambalavanan N, McMahon LL. Vitamin A and retinoic acid combination attenuates neonatal hyperoxia-induced neurobehavioral impairment in adult mice. *Neurobiol Learn Mem* 2017;141:209–16.
42. Ramani M, van Groen T, Kadish I, Bulger A, Ambalavanan N. Neurodevelopmental impairment following neonatal hyperoxia in the mouse. *Neurobiol Dis* 2013;50:69–75.
43. Schmitz T, Endesfelder S, Reinert MC, Klinker F, Müller S, Bühner C, et al. Adolescent hyperactivity and impaired coordination after neonatal hyperoxia. *Exp Neurol* 2012;235:374–9.
44. Quinn LP, Perren MJ, Brackenborough KT, Woodhams PL, Vidgeon-Hart M, Chapman H, et al. A beam-walking apparatus to assess behavioural impairments in MPTP-treated mice: pharmacological validation with R(-)-deprenyl. *J Neurosci Methods* 2007;164:43–9.
45. Yokoi F, Chen HX, Dang MT, Cheetham CC, Campbell SL, Roper SN, et al. Behavioral and electrophysiological characterization of Dyt1 heterozygous knockout mice. *PLoS One* 2015;10:e0120916.
46. Bradl M, Lassmann H. Oligodendrocytes: biology and pathology. *Acta Neuropathol* 2010;119:37–53.